

A CANDIDATE PROTOPLANET IN THE TAURUS STAR-FORMING REGION

S. TEREBEY,¹ D. VAN BUREN,² D. L. PADGETT,² T. HANCOCK,¹ AND M. BRUNDAGE²

Received 1998 July 9; accepted 1998 August 18; published 1998 September 30

ABSTRACT

Hubble Space Telescope/Near-Infrared Camera and Multiobject Spectrometer images of the class I protostar TMR-1 (IRAS 04361+2547) reveal a faint companion with $10''0 = 1400$ AU projected separation. The central protostar is itself resolved as a close binary with $0''31 = 42$ AU separation, surrounded by circumstellar reflection nebulosity. A long narrow filament seems to connect the protobinary to the faint companion TMR-1C, suggesting a physical association. If the sources are physically related, then we hypothesize that TMR-1C has been ejected by the protobinary. If TMR-1C has the same age and distance as the protobinary, then current models indicate that its flux is consistent with a young giant planet of several Jovian masses.

Subject headings: binaries: general — circumstellar matter — infrared: stars — planetary systems — stars: formation — stars: individual (TMR-1)

1. INTRODUCTION

The past few years have seen the indirect detection by their gravitational effects of roughly one dozen extrasolar Jupiter-mass planets around nearby stars (Marcy & Butler 1998). Doppler surveys are primarily sensitive to giant planets within 3 AU of the central star, posing a challenge to theories that predict birthplaces in the 5–10 AU range. The conventional picture proposes a two-step formation process in which a rocky planet core forms in a disk, followed by gas accretion over a period of $(1\text{--}10) \times 10^6$ yr in a region outside 5 AU radius (Lissauer 1995). An alternative theory argues that giant planets form via gravitational instabilities in the disk on a timescale of thousands rather than millions of years (Boss 1998).

We have detected a low-luminosity object near the class I protostar TMR-1 whose flux is consistent with that of a giant protoplanet. If confirmed, the protostar's age of approximately 300,000 yr places severe constraints on the timescale of giant planet formation. Furthermore, the data show that the TMR-1 protostar is a binary system. Most stars are members of multiple star systems with separations ranging widely from less than 1 AU to thousands of AU; the overlap with circumstellar disk sizes has consequences for planet formation (Benet 1996; Bate & Bonnell 1997). An important issue is whether binary stars provide a hospitable environment for the formation of substellar mass objects.

2. TMR-1 PROTOSTARS

Previous observations establish TMR-1 as a typical class I protostar, similar in mass and luminosity to the Sun, having $\sim 0.5 M_{\odot}$ and $3.8 L_{\odot}$, respectively, and which millimeter observations suggest has a low-mass disk (Bontemps et al. 1996). Observed near-infrared (NIR) magnitudes are $J = 16.1$, $H = 12.9$, and $K = 10.6$ (Terebey et al. 1990; Kenyon et al. 1993). Class I protostars are surrounded by opaque envelopes of infalling gas and dust. Based on statistical and theoretical arguments, typical ages of class I protostars are 100,000–300,000 yr (Terebey et al. 1984; Shu, Adams, & Lizano 1987). NIR imaging and millimeter interferometry data of TMR-1 show a bipolar outflow that extends southeast to northwest (Terebey et al. 1990; Hogerheijde et al. 1998). Based on the arguments

given in Chandler et al. (1996), TMR-1 is not viewed edge-on or pole-on, but at an intermediate ($\sim 60^\circ$) inclination.

3. HUBBLE SPACE TELESCOPE NEAR-INFRARED CAMERA AND MULTIOBJECT SPECTROMETER IMAGES AND PHOTOMETRY

The high spatial resolution ($0''.15$ at $1.6 \mu\text{m}$) *Hubble Space Telescope* (HST)/Near-Infrared Camera and Multiobject Spectrometer (NICMOS) images in Figure 1 resolve the TMR-1 protostar into two point sources which we call A and B (A is the northern component). At the Taurus cloud distance of 140 pc, the $0''.31$ projected separation is 42 AU, a fairly typical binary separation. The new data reveal TMR-1 to be a protobinary surrounded by gas and dust, viewed during the epoch of formation.

Figure 1 displays extensive nebulosity, which is brightest near the protobinary. A long narrow filament extends in a gentle curve from near the protobinary to a third fainter point source, which we call C, located $10''0$ southeast. The image provides strong visual evidence that object C appears associated with the protobinary by means of the filament. TMR-1C is detected at a signal-to-noise ratio (S/N) of 50 in the F205W filter, as implied by the presence of the Airy diffraction ring.

The image artifacts (Casertano et al. 1997)³ are easily identified in the original image orientation ($+y$ -axis at P.A. = 38° east of north). Artifacts arising from the bright protostars include the $\pm 45^\circ$ telescope diffraction spikes, electronic ghost stars at ± 128 pixels along the (x, y) -axes, and two faint electronic ghost columns, one of which passes through the protostars and another seen 128 pixels to the left. Finally, a residual coronagraphic spot appears in the upper left-hand quadrant.

Extended nebulosity is common around protostars at NIR wavelengths. Stellar photons escape through the transparent polar regions created by the bipolar outflow; they delimit the $\tau \sim 1$ surface when they absorb or scatter in the dusty infall envelope and dusty circumstellar disk (Whitney, Kenyon, & Gomez 1997). The highly structured nebulosity around the TMR-1 protostars implies that the density is inhomogeneous. The sharp contrast of the filament above the background suggests that the density is locally enhanced, while the illumination of the filament at large ($10''$) distances suggests a fairly clear line of sight back to the protostars.

¹ Extrasolar Research Corporation, 569 South Marengo Avenue, Pasadena, CA 91101.

² Jet Propulsion Laboratory, IPAC 100-22, Caltech, Pasadena, CA 91125.

³ Papers submitted for the proceedings are available on-line at http://ica-rus.stsci.edu/~stefano/Papers_final_pdf.html.

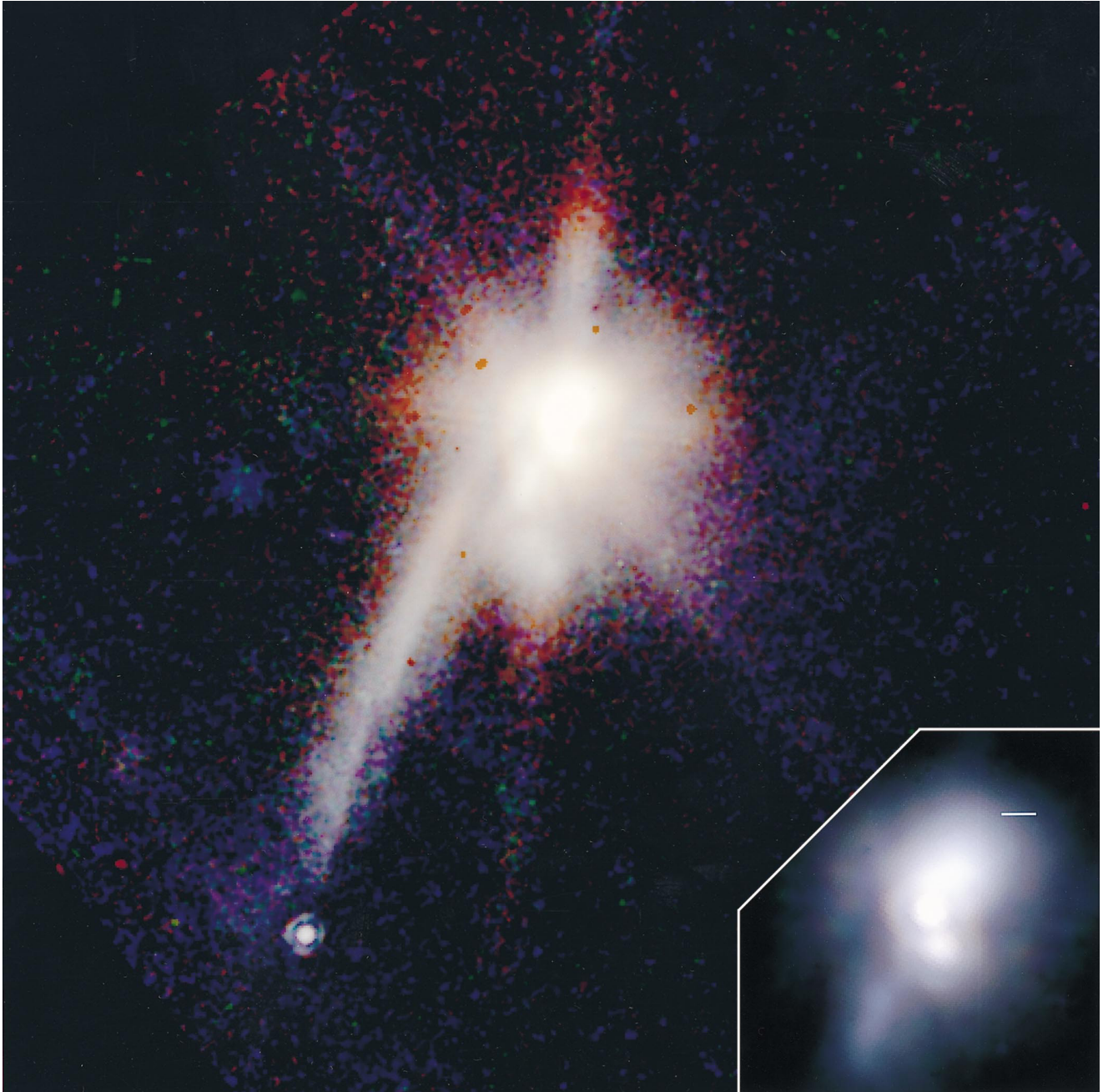


FIG. 1.—True-color *HST*/NICMOS image of protostar TMR-1 with 256 pixels = $19''.4$ field of view. There is a long narrow filament extending from the protobinary to a faint point source which is the candidate protoplanet. The inset shows a magnified view ($0''.3 = 42$ AU scale) of the protobinary in the central region, complete with first Airy diffraction ring around each component. The field is suffused by bright nebulosity. The region is heavily reddened, but short wavelengths have been boosted to make the nebulosity appear white. Shown are the F205W filter ($2.05\ \mu\text{m}$) in red, the F187W filter ($1.87\ \mu\text{m}$) in green, and the F160W filter ($1.60\ \mu\text{m}$) in blue; north is up. The display uses log stretch.

Table 1 gives positions and individual component fluxes via point-spread function (PSF) fitting. Fluxes based on aperture photometry are given in Table 2 both to facilitate comparison with ground-based measurements and to place the data on the STScI *HST*/NICMOS photometric system. Ground-based $2.2\ \mu\text{m}$ *K*-band Infrared Telescope Facility (IRTF) images and also K' at Keck (G. Blake 1998, private communication; Hogerheijde et al. 1998) confirm the detection and approximate flux of object C.

4. LOCAL NIR STAR COUNTS, CHANCE BACKGROUND OBJECT, AND EXTINCTION

For the Taurus cloud *K*-band star counts give $N(K' <$

$K) = 0.041 \times 10^{0.32K}$ stars deg^{-2} , which includes an extinction of $A_K = 0.4$ estimated from the same data (Beichman & Jarrett 1994). Assuming 18.5 for the *K*-band magnitude implies about one background star per NICMOS frame.

A posteriori probability estimates are problematic. However, we press on, noting that the TMR-1 filament is a unique structure in our ensemble of *HST*/NICMOS images. The chance that a random background star lies at the tip of the filament is 2% if we assign a conservatively large $3'' \times 3''$ effective search area.

The scarcity of background stars is empirically confirmed by the *HST* data, which show fewer than expected background stars because of high extinction local to the protostars. Com-

TABLE 1
TMR-1 *HST*/NICMOS POSITIONS^a AND PHOTOMETRY^b

Component	R.A. (J2000)	Decl. (J2000)	F160W 1.60 μm	F187W 1.87 μm	F205W 2.05 μm
A	04 39 13.84	25 53 20.6	38^{+22}_{-20}	53^{+10}_{-11}	250^{+80}_{-70}
B	04 39 13.83	25 53 20.4	9^{+17}_{-9}	23.5^{+8}_{-8}	180^{+70}_{-117}
C	04 39 14.14	25 53 11.8	$1.17^{+0.06}_{-0.04}$	$0.98^{+0.05}_{-0.04}$	$3.32^{+0.20}_{-0.20}$

NOTE.—Units of right ascension are hours, minutes, and seconds, and units of declination are degrees, arcminutes, and arcseconds.

^a 0".35 = 1 σ *HST* absolute position error.

^b PSF amplitude fitting and 1 σ limits in counts s⁻¹ image units. Limits are instrumental for C and dominated by background structure for A and B. Absolute photometry errors of 3% should be added in quadrature. To convert units to microjanskys, but applying no color correction, multiply by 15.6, 34.4, and 12.4 for F160W, F187W, and F205W filters, respectively.

parable S/N *HST*/NICMOS images for nine class I protostars in Taurus show one other secondary object ($K = 18.7$ mag), giving one or two possible background objects in nine fields. To match the large-scale NIR star counts implies an average extinction over the 20" NICMOS field of view of $A_K = 1-2$ ($A_V = 10-20$) toward class I protostars in Taurus.

An alternate estimate for the extinction is set by values previously derived for the protostar, which range from 2.5 to 4 at K (Terebey et al. 1990; Whitney et al. 1997). The extinction is likely smaller at 10" distance from the protostar, as is also suggested by the Table 1 flux ratios. Intrinsic NIR stellar colors are near zero because the spectral energy distribution of many stars is near the Rayleigh-Jeans limit. The observed highly reddened colors of protostars are therefore caused by extinction and scattering. The increasing flux ratio of object C relative to either protostar suggests there is less extinction toward object C than toward A and B.

5. LUMINOSITY AND TEMPERATURE

Models of giant planets and brown dwarfs imply that they are hottest and brightest when young, as luminous as $0.01 L_\odot$ at 1×10^6 yr (Nelson, Rappaport, & Joss 1993; Burrows et al. 1997). The radii are near that of Jupiter's, $R_J = 7.1 \times 10^9$ cm, over a large mass and temperature range; young objects should be modestly (up to a factor of 3) larger. Models suggest effective temperatures as great as 3000 K below 1×10^6 yr of age.

The object TMR-1C is clearly much fainter than the neighboring protostars; if located at the same distance as the Taurus cloud, then the estimated bolometric luminosity is approximately 10^{-3} to $10^{-4} L_\odot$, within the giant planet-to-brown dwarf regime. To derive its luminosity, the observed NIR fluxes were fit assuming for simplicity a blackbody spectrum extinguished by dust. Dust extinction parameters are from B. Draine (1998, private communication). Assumptions are 140 pc distance, $1 R_J$ minimum radius for stellar and substellar objects, and $A_V < 30$ ($A_K < 3$) extinction. The extinction cap is selected as the maximum compatible with NIR background source counts (§ 4).

General results from varying T_{eff} , A_V , and radius are that the temperature is not well constrained, since values ranging from 1200 K ($A_V = 0$) to 3000 K ($A_V = 30$) give acceptable fits. However, the radius is reasonably constrained to be a few R_J at the assumed distance and depending also on the maximum extinction at the high-temperature end. Relaxing our assumptions, hotter background stars provide acceptable fits if higher extinctions are allowed. Foreground stars or low extinctions are ruled out; the approximate $H - K$ color of 1.5 is redder than the photospheres of known low-luminosity stars.

TABLE 2
FLUX OF TMR-1C^a

BAND/FILTER	FLUX	
	μJy	mag
<i>R</i>	>22.2 ^b
<i>J</i>	>21.2 ^c
F160W	16.	19.6
F187W	33.	18.5
F205W	39.	18.2
<i>K</i>	17.9 ^c
<i>L</i>	>13.2 ^c

^a NICMOS magnitudes are based on standard 0".5 apertures and the *HST* Vega system. Background structure dominates the 10% photometric uncertainty.

^b 5 σ limit from Jarrett, Dickman, & Herbst 1994.

^c 1998 April IRTF NSFCAM data. *K* band has 20% photometric uncertainty; 3 σ limits elsewhere.

The broadband NICMOS filters give limited spectral information but allow us to exclude effective temperatures below approximately 1600 K since there is no evidence in TMR-1C for a strong methane dip near $1.8 \mu\text{m}$ (e.g., Allard & Hauschildt 1995). NIR spectra of cool objects (~ 2000 K) which show water at $1.9 \mu\text{m}$ are sufficiently featureless to be consistent with our photometry (e.g. Fig. 7 of Oppenheimer et al. 1998). Better constraints on the extinction and effective temperature await low-resolution spectra of TMR-1C.

6. MASS

Model evolutionary tracks for giant planets and brown dwarfs show that the derived mass depends strongly on the age and luminosity (Fig. 7 of Burrows et al. 1997). If TMR-1C has the same 300,000 yr age assumed for the protostars, then A_V is 8–20 and the mass is 2–5 M_J . If the age is 10×10^6 yr, the same as older pre-main-sequence stars in Taurus, the mass may be as high as 15 M_J . However, below 1×10^6 yr, the models are sensitive to the initial conditions, since the thermal relaxation timescale is comparable to the planet's age. More realistic models will depend on the planetary formation mechanism.

7. EJECTION HYPOTHESIS

If TMR-1C is a physical companion of the TMR-1 binary, then models suggest that it formed much closer to the protostars than its observed 1400 AU projected distance. We hypothesize that TMR-1C has been ejected by the two protostars. Apart from some exceptions such as hierarchical systems, celestial dynamics finds that three-body stellar systems with comparable separations are unstable and tend to eject the lowest mass object (Monaghan 1976). On dimensional grounds the characteristic velocity of ejection is $(GM/R)^{0.5}(1+e)$, the velocity of periastron passage of the binary. Numerical studies show a large dispersion in ejection velocities (Standish 1972).

The separation of the protostars allows us to estimate a characteristic ejection velocity. The computation is only indicative given that the orbital parameters and inclination are poorly known. The observed projected separation of stars A and B is 42 AU; statistically, binaries spend the most time at the widest separations. For a typical binary eccentricity of $e = 0.5$, the separation varies by a factor of 3. Including a modest deprojection correction, periastron passage may occur at 15–30 AU separation. The corresponding ejection velocity is 5–10 km s⁻¹ for $1 M_\odot$ assumed total mass. The current distance of 10" then implies that the time since ejection is about 1000 yr.

Consider for the moment that the filament marks the trail of

object C. The filament's shape is curved and appears consistent with the expected hyperbolic trajectory. However, shear is likely important if the filament lies within the differentially rotating infall envelope or disk. The assumption of Keplerian rotation is adequate to estimate the timescale (Terebey et al. 1984). The period is 1000 yr at 100 AU radius, which implies that significant wrapping can be expected on roughly 0".67 size scales.

8. FILAMENT

Although the position angles of the filament and outflow are similar, the filament differs from typical NIR outflow structures. Models of outflow cavities show conical shapes (Whitney et al. 1997); if the outflow cavity is limb-brightened, it should have two symmetric horns with a sharp outer edge, whereas what is observed is one filament whose sharp edge is on the wrong (southern) side given its curvature. NIR polarimetry data show that the filament is primarily scattered stellar light emanating from the protostars (Lucas & Roche 1997), which rules out an emission-line jet.

The filament is projected against the outflow, but the moderate source inclination implies that the filament could traverse either the outflow cavity or the dense infall envelope. One possible explanation is that the filament may be a material tail, such as, for example, a tidal tail formed by two colliding circumstellar disks (Lin et al. 1998). Ground-based data in support of a material tail show HCO^+ along the filament, indicating the presence of dense gas (Hogerheijde et al. 1998). However, HCO^+ can be ambiguous as a dense gas tracer because it often has enhanced abundance in molecular outflows. Alternatively, the filament may be an illumination channel, or light pipe, created when the protoplanet tunneled through the infall envelope. A drawback to the light-pipe explanation is that Bondi-Hoyle gravitational accretion implies a diameter that is too narrow to explain the observed filament, so some other mechanism must operate.

9. ISOLATED PLANETS

We have proposed that TMR-1C is a substellar object that has been ejected by a binary protostar. There are two key

experiments to test the idea that TMR-1C is an ejected protoplanet. Spectra will measure the extinction and effective temperature to better discriminate between stellar, brown dwarf, or planet origin. In several years, proper motion measurements will detect TMR-1C's motion on the sky. The predicted direction may be along the filament, or in the case of a tidal tail, at an angle to the filament (Lin et al. 1998).

We outline one of the many possible mechanisms for planet ejection. Three-body numerical simulations suggest that stable planetary orbits exist at radii approaching half the binary periastron separation (Benest 1996). In other words, there is a maximum stable radius for planet formation in a binary system. A substellar object that migrates or forms in the zone of marginal stability is subject to orbital resonance pumping. After repeated periastron passages, the object gains sufficient energy to escape the system. This mechanism does not require a gaseous disk per se and so may apply to pre-main-sequence stars as well as to protostars.

The discovery of an ejected protoplanet is unexpected. However, given the prevalence of binary systems the process seems inevitable, and the question becomes how often. The idea that young planets should occasionally be ejected from their solar systems is rich in implications, both for our understanding of how planetary systems form and in strategies for detecting isolated planets using current technology.

Many people provided support or encouragement. A special thanks to Charlie Lada for pointing out that brown dwarfs would have a K -magnitude near 17 in Taurus. We thank John Rayner and Bob Joseph for providing Infrared Telescope Facility observations on short notice. S. T. gratefully acknowledges NASA support including NASA Origins of Solar Systems Program funding under contract NASW-97009 and funding from grant GO-07325.01-96A through the Space Telescope Science Institute, which is operated by the Association of Universities for Research in Astronomy, Inc. under NASA contract NAS5-26555. This work was carried out in part at the Jet Propulsion Laboratory, operated by the California Institute of Technology under contract for NASA.

REFERENCES

- Allard, F., & Hauschildt, P. H. 1995, *ApJ*, 445, 433
 Bate, M. R., & Bonnell, I. A. 1997, *MNRAS*, 285, 33
 Beichman, C. A., & Jarrett, T. 1994, *Ap&SS*, 217, 207
 Benest, D. 1996, *A&A*, 314, 983
 Bontemps, S., André, P., Terebey, S., & Cabrit, S. 1996, *A&A*, 858
 Boss, A. P. 1998, *Nature*, 393, 141
 Burrows, A., et al. 1997, *ApJ*, 491, 856
 Casertano, S., Jedrzejewski, R., Keyes, T., & Stevens, M., eds. 1997, *Proc. 1997 HST Calibration Workshop with a New Generation of Instruments* (Baltimore: STScI)
 Chandler, C. J., Terebey, S., Barsony, M., Moore, T. J. T., & Gautier, T. N. 1996, *ApJ*, 471, 308
 Hogerheijde, M. R., van Dishoeck, E. F., Blake, G., & van Langevelde, H. J. 1998, *ApJ*, 502, 315
 Jarrett, T. H., Dickman, R. L., & Herbst, W. 1994, *ApJ*, 424, 852
 Kenyon, S. J., Whitney, B. A., Gomez, M., & Hartmann, L. 1993, *ApJ*, 414, 773
 Lin, D. N. C., Laughlin, G., Bodenheimer, P., & Rózycka, M. 1998, *Science*, in press
 Lissauer, J. J. 1995, *Icarus*, 114, 217
 Lucas, P. W., & Roche, P. F. 1997, *MNRAS*, 286, 895
 Marcy, G. W., & Butler, R. P. 1998, *ARA&A*, 36, 57
 Monaghan, J. J. 1976, *MNRAS*, 176, 63
 Nelson, J. A., Rappaport, S., & Joss, P. C. 1993, *ApJ*, 404, 723
 Oppenheimer, B. R., Kulkarni, S. R., Matthews, K., & van Kerkwijk, M. H. 1998, *ApJ*, 502, 932
 Shu, F. H., Adams, F., & Lizano, S. 1987, *ARA&A*, 25, 23
 Standish, E. M. 1972, *A&A*, 21, 185
 Terebey, S., Beichman, C. A., Gautier, T. N., & Hester, J. J. 1990, *ApJ*, 362, L6
 Terebey, S., Shu, F. H., & Cassen, P. 1984, *ApJ*, 286, 529
 Whitney, B. A., Kenyon, S. J., & Gomez, M. 1997, *ApJ*, 485, 703

Note added in proof.—The paper “Spectroscopy of Brown Dwarf Candidates in the ρ Ophiuchi Molecular Core” by B. A. Wilking, T. P. Greene, and M. R. Meyer (*AJ*, in press [1998]) describes NIR spectroscopy and NIR colors that are relevant to the case of TMR-1C.